Middle-East Journal of Scientific Research 23 (8): 1969-1979, 2015
ISSN 1990-9233

DOI: 10.5829/idosi.mejsr.2015.23.08.220

Inverse Heat Transfer Method, Application: Achieving Constant Heat Flux on Flatplate by Using Impinging Slot-Jet Arrays and Experimental Estimation of Convective Heat Transfer Coefficient

S.D. Farahani, F. Kowsary, M. Ashjaee and H. Nikpay

Department of Mechanical Engineering, College of Engineering, University of Tehran, Tehran, Iran

Abstract: A numerical algorithm is developed to obtain an optimized array of four laminar impinging slot jets for achieving constant convective heat transfer coefficient on flat plate. Root mean square deviation of the local Nusselt distribution from the desired Nusselt number is considered as the objective function. Jets' widths, jet-to-jet and jet-to-surface spacing's and the overall flow rate are chosen as design variables. Conjugate gradients method along with backtracking line search is applied to optimize the objective function calculated by numerical simulation for three different cases of Nu=7, 9 and 11. For each of these desired Nusselt numbers, an almost uniform distribution of local Nusselt number with percent of root mean square error less than 2.5% is achieved in fewer than 12 iterations. An experimental study using inverse heat conduction method has been performed. The inverse method is conjugated gradient method with adjoint equation. In this experiment, only temperatures histories in target plate is measured. The measured distribution of local Nusselt number is in good agreement with numerical results in all three optimal configurations.

Key words: Uniform Nusselt number · Impinging slot jet array · Inverse method · Conjugated gradient method · Adjoint equation

INTRODUCTION

Heat flux uniformity is an important requirement in many different applications in metal, glass, food and electronic industries where uniform heating or cooling is necessary to ensure material quality or to enhance performance. Roetzel and Newman [1] developed a wall profile which yields a uniform overall heat transfer resistance of wall and condensate film in order to obtain uniform heat flux in paper drying drums. Sparrow and Carlson [2] investigated heat flux uniformity at thin, electrically heated metallic foils. Birla *et al*. [3] improved heating uniformity of fresh fruit in radio frequency treatments. Rafidi and Blasiak [4] investigated the effect of the HiTAC flame characteristics on the heat transfer intensity and uniformity inside a test furnace. Zareifard *et al*. [5] developed a mathematical method to produce uniform heat flux in industrial ovens. Chander and Ray [6] conducted an experimental study on three interacting methane/air flame jets impinging normally on a flat surface and examined the effect of different parameters on heat flux uniformity.

Heat flux uniformity is also a common problem in inverse heat transfer. In previous researches, all three modes of heat transfer have been used in order to accomplish this purpose. However most of them employed radiation heat transfer because of its better controllability in heating, although it does not offer the same advantage in cooling.

Impinging jets are widely used in heating or cooling of solid surfaces where high intensity heat fluxes are desired. Directed flow of fluid targeted at the design surface can transfer large amounts of heat, therefore given a required Nusselt number, the flow Reynolds number maybe very smaller than that required for other convective cooling approaches. In addition, concentration of heat transfer in impinging jets makes it possible to control the heat flux distribution by altering parameters such as jet-to-jet spacing in both heating and cooling.

Corresponding Author: S.D. Farahani, Department of Mechanical Engineering, College of Engineering, University of Tehran, P.O. Box: 11155-4563, Tehran, Iran.
Tel: +9821-61114024, Fax: 9821-88013029.

Research on this type of convective heat transfer has resulted in a large amount of literature during the past years. Martin [7] and Zuckerman [8] reviewed this literature. Gardon and Akfirat [9] used experimental data to correlate both local and average heat transfer coefficients with Re, Prandtl number, jet-to-surface distance and jet diameter for single and multiple two-dimensional air jets impinging on an isothermal surface. They investigated the effect of the interaction between jets on the uniformity of heat transfer in various arrangements.

Huber and Viskanta [10] conducted experiments on impinging arrays of axisymmetric confined air jets. They studied the effect of jet-to-jet spacing, nozzle-to-plate distance and spent. air exits on the magnitude and uniformity of the convective heat transfer coefficient. They acheived a more uniform distribution of Nusselt number when large fraction of the impingement surface was covered by the stagnation region and the effect of the low convection coefficients corresponding to the wall jet region were minimized. Wadswoth and Mudawar [11] performed an experimental study to remove heat from electronic chips using a confined two-dimensional slot jet. They concluded that two-dimensional jets produced larger impingement regions leading to better cooling effectiveness and provided more uniformity and controllability. Wang *et al*. [12] carried out experiments to control the jet impingement heat transfer in cross flow. They stated that using a rib leads to more heat transfer uniformity. Na-pompet and Boonsupthip [13] employed impinging slot jets with narrow channels to achieve more uniform heat flux. San and Chen [14] studied the effects of jet to plate distances and jet-to-jet spacing's on the distribution of the Nusselt number for different configurations of staggered jet arrays. They observed a more uniform Nusselt distribution at large jet to plate spacing's.

There are numerous published works on jet impingement cooling which have been concerned with heat flux uniformity [15]. However, none have attempted to come up with a mathematically optimized solution. As mentioned above, using multiple slot jets improves uniformity and controllability of heat flux over the heated surface and provides a more effective cooling performance compared to the single slot and round jets. Though, turbulent impinging jets are more common in industrial applications, laminar jets are employed in cooling of more fragile components like electronic modules. This work focuses on two subjects: inverse design of impinging slot jet arrays to obtain heat flux uniformity in the laminar range and experimental estimation local heat transfer coefficient using inverse heat conduction method. Estimation of convective heat transfer coefficient is nonlinear. Thus, conjugated gradient method with adjoint equation was used in this study.

Problem Description: An array of four slot jets is used to generate uniform heat flux along the target surface. The flow domain is considered to be symmetric with respect to the y axis in order to reduce the computational effort. The schematic of impinging jets, target surface and boundary conditionsare depicted in Fig. 1. Rate of heat transfer at the target surface is characterized by the Nusselt number (Nu),

$$Nu = \frac{hD_h}{k} \tag{1}$$

In the case of slot jets, the hydraulic diameter (D_h) is replaced by $2w$, where w is the slot width. Another important parameter in impinging jets is the Reynolds number,

$$\mathrm{Re} = \frac{vD_h}{\nu_e} \tag{2}$$

where v_e is the initial average flow speed at the nozzle exit and ν is the fluid viscosity. The coolant is ambient air. The flow domain is considered to be two-dimensional. Assuming incompressible, steady, laminar flow and neglecting viscous dissipation and radiation heat transfer, the non-dimensional continuity, momentum and energy equations in the Cartesian system are:

$$\frac{\partial u}{\partial x} + \frac{\partial v}{\partial y} = 0 \tag{3}$$

$$\rho(u\frac{\partial u}{\partial x} + v\frac{\partial u}{\partial y}) = -\frac{\partial p}{\partial x} + \mu[\frac{\partial^2 u}{\partial x^2} + \frac{\partial^2 u}{\partial y^2}] \tag{4}$$

$$\rho(u\frac{\partial v}{\partial x} + v\frac{\partial v}{\partial y}) = -\frac{\partial p}{\partial y} + \mu[\frac{\partial^2 v}{\partial x^2} + \frac{\partial^2 v}{\partial y^2}] - \rho g \tag{5}$$

$$\rho c_p(u\frac{\partial T}{\partial x} + v\frac{\partial T}{\partial y}) = k[\frac{\partial^2 T}{\partial x^2} + \frac{\partial^2 T}{\partial y^2}] \tag{6}$$

System of conservation equations for continuity, momentum and energy are solved numerically using the finite volume method [16] in order to calculate the distribution of local Nusselt number along the target surface. The first order upwind scheme is used for the advective terms and the pressure-velocity coupling is resolved using the SIMPLE algorithm [17]. The flow domain is divided into a set of square blocks and each of

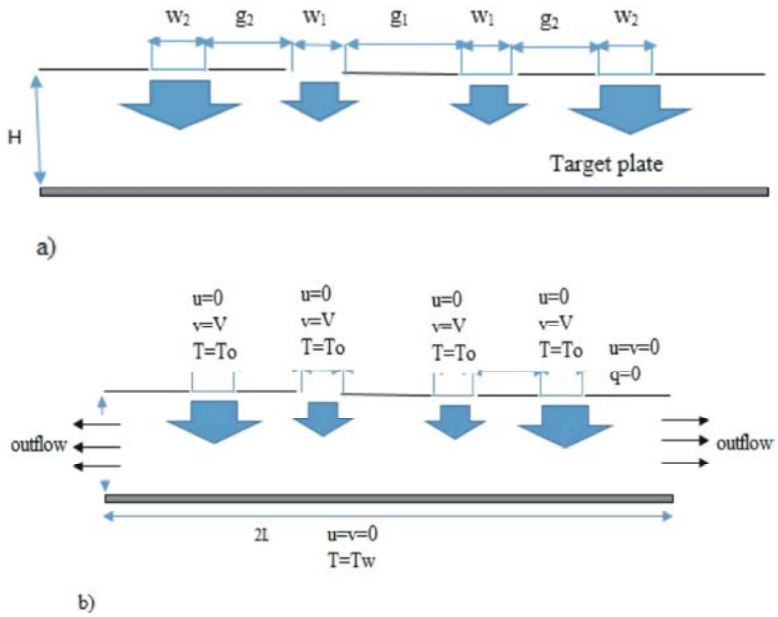

Fig. 1: a) Schematic of the array of slot jets b) boundary condition

these regions is discretized using a structured mesh. The grid is refined near the target surface. In order to both guarantee the numerical accuracy and reduce the computational cost of the inverse design procedure, the grid independence is studied by employing different fine and coarse meshes and the optimum grid size is determined. The grid refinement is continued until halving the grid size resulted in less than 1% change in the magnitude of the objective function, as defined later, while the computational cost is eight folded. The grid is adaptive to the geometry change during every iteration of the optimization algorithm. Moreover, grid refinements showed no more improvements at the optimal arrangements. The numerical results are considered to be converged when normalized residuals of conservation equations become less than (10^{-6}).

Rearranging inverse design problems into external formulations and employing numerical methods of the optimization theory is a common practice in the field of inverse heat transfer [18, 19]. The main objective of this research is to generate uniform heat flux, or in other words, to have a uniform distribution of local Nusselt number along the target plate. In order to accomplish this purpose, summation of the calculated Nusselt numbers deviation from the desired Nusselt number (Nu_d) should be minimized, therefore the root-mean-square error (E_{rms}) is used as the objective function.

$$E_{rms} = \sqrt{\frac{1}{N}\sum_{i=1}^{N}\left(\frac{Nu_d - Nu_i}{Nu_d}\times 100\right)^2} \qquad (7)$$

The volumetric flow rate (Q), two jet-to-jet spacings (g_1, g_2), two slot widths (w_1, w_2) and jet-to-surface spacing (h) are taken as design variables. These variables may be re-written in non-dimensional form as the Reynolds number (Re), W_1 (=w_1/D_h), W_2(=w_2/D_h), G_1(=g_1/D_h), G_2(=g_2/D_h), and H(=h/D_h). The upper and lower bounds of the geometrical design variables are as follows,

$2mm \le w_i \le 10mm$ (i=1,2)

$2mm \le g_i \le 8mm$ (i=1,2)

$14mm \le h \le 70mm$ (8)

The nonlinear conjugate gradients method is employed for minimizing the objective function. It is an elegant numerical algorithm originally introduced by Hestenes and Stiefel [20] for solving sparse systems of linear equations. The method of conjugate gradients was generalized to nonlinear optimization problems by Fletcher and Reeves [21]. This technique performs a line search along the proposed direction in each iteration. In the current study, exact form of the objective function is not available and its value is calculated using CFD simulations. Therefore, Backtracking line search method is implemented to find the proper step size in each iteration. Details of this inexact line search method can be found in [22].

The iterative inverse design algorithm consists of the following steps:

- Starting with an initial guess for six design variables
- Calculation of the objective function and it's gradient at the initial condition by solving the direct problem
- Finding the search direction using the Fletcher-Reeves nonlinear conjugate gradient method
- Calculation of the optimal step size along the search direction using the Backtracking technique
- Determination of a new set of design variables
- Testing for the convergence of the iterative algorithm
- If the solution has been converged, terminating the process, otherwise going back to step 2.

Experimental Setup and Procedure: A schematic of the experimental apparatus is shown in Fig. 2. Compressed air flows through a series of two air filters, an air filter/regulator and then a flow meter (Rotameter) into a plenum chamber. A pressure gauge, connected before the plenum chamber, is used to correct the flow rate. Baffle plate in the inlet of the plenum chamber allows the flow to decelerate and expand. A row of stainless steel mesh screen and honeycomb, which is used to produce uniform velocity profile at the nozzle outlets, are mounted in the bottom half of the plenum chamber in order to dissipate large and small eddies, respectively. A programmable 3-D stage controller, used to adjust the position of the hot-wire sensor, can be positioned at the right measuring place within 15 ìm spatial resolution; The most deviations of the mean velocity between I-type hot wire sensor and rotameter are 0.4% for all cases. Top of plexiglass plenum's surface is screwed to the other plexiglass plates which contact zones are sealed with rubber gaskets and silicon glue to prevent any probable air leakage. The jet nozzle is placed at the bottom of the plenum chamber. The length of two- dimensional slot jet is considered longer than the target plate to avoid the entrance of three-dimensional vertical structures of slot corner into the heated zone. The dimension of nozzle is calculated by optimization for every case study.A stainless steel (AISI-304) plate 250 × 70 ×5 mm^3 was used as a target surface. A silicon heater of less than 3 mm thickness, placed at the bottom of the plate provides a uniform heat flux of 2000 W/m^2. The total power supplied was monitored using two digital multi-meters which one was used for voltage and the other for the current was used. The emissivity of the plate surface, which is polished by grinding process to minimize the radiation heat transfer, is measured 0.75 via an infrared thermometer gun. Wooden end caps with thermal conductivity of 0.12W/m.K are attached to small sides of the plate to minimize the end effects.

The surface temperatures in target plate were measured over a distance of seven times the slot width from the stagnation point. We used 11 type-K thermocouples, one at the stagnation point, 9 on the left hand side and 1 on the right side of the symmetry line to check the symmetry of the heat transfer distribution. Distance between each two adjacent thermocouples is 3 mm. Three layers of materials were used to insulate the backside of the target plate and the heater assembly. The first layer was a wood insulation of 16mm thickness, (thermal conductivity 0.12W/(m.K)), the second layer was a fiber glass of 12 mm thickness, (thermal conductivity 0.035W/(m.K)) and the third layer was a elastomer of 6mm thickness (thermal conductivity 0.036 W/(m.K)). Thermocouples were inserted through holes of 4.5 mm depth machined through the thickness of the plate. The wood-heater surface temperatures in target plate were measured using 11 type-K thermocouples, with same arrangement on wood surface. Using the thermocouples in wood, heat flux's heater was estimated exactly to ensure the value of it is true.

The convective heattransfer coefficients have been estimated by using the real measured temperatures in plate and inverse method. In our experimental study, the inverse method was conjugate gradient method with adjointequation [23] due to estimation of convective heat transfer coefficient is nonlinear. Using this method convective heat transfer is estimated directly. The physical model for target plate is defined as (Fig. 3):

$$\frac{\partial^2 T}{\partial x^2}+\frac{\partial^2 T}{\partial y^2}=\frac{1}{\alpha}\frac{\partial T}{\partial t}$$
$$\frac{\partial T}{\partial x}\Big|_{x=0}=\frac{\partial T}{\partial x}\Big|_{x=L}=0$$
$$-k\frac{\partial T}{\partial y}\Big|_{y=0}=q \qquad (9)$$
$$-k\frac{\partial T}{\partial y}\Big|_{y=E}=h(T-T_{jet})\ +\varepsilon\sigma(T^4-T^4_{\ jet})\ and\ T\Big|_{t=0}=T_0$$

where q is heat flux of heater, h is unknown. Heat transfer in target plate was considered two dimensional In order to estimate the heat transfer coefficient by using the conjugate gradient method, the error function S is defined as:

$$S(h)=\sum_{i=1}^{N_s}\sum_{m=1}^{N_m}(T_i(t_m)-Y_i(t_m))^2 \qquad (10)$$

where Y is measured temperatures at sensor locations and Tis the estimated value at sensor locations in heat equation. The directional derivative of S for nonlinear problems is obtained from the adjoint equation.

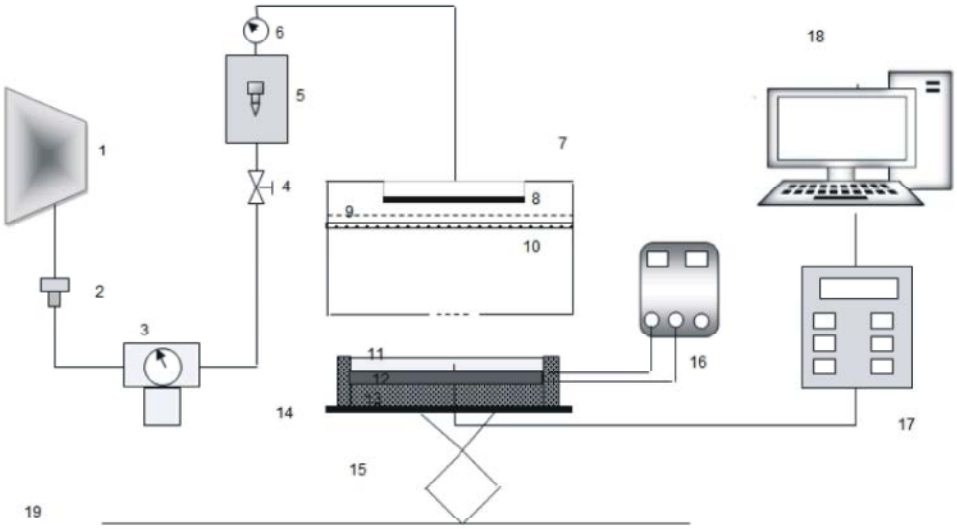

Fig. 2: Experimental setup

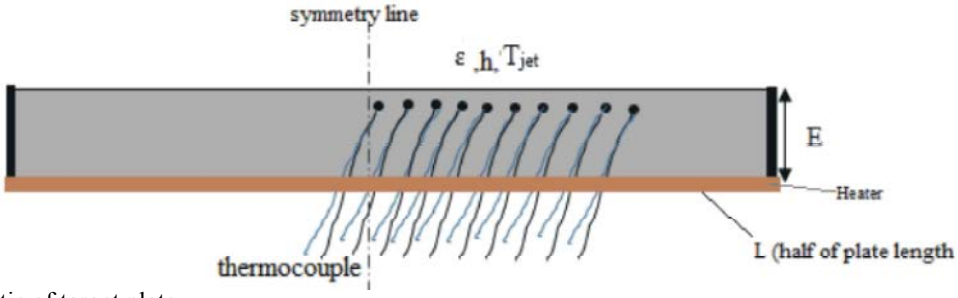

Fig. 3: Schematic of target plate

$$\vec{\nabla} S = \frac{\partial S}{\partial h} dh \tag{11}$$

where all the mentioned parameters are evaluated at the sensor locations.Using the above equation, the conjugate direction (d) can be calculated as

$$d^k = \nabla S(h^k) + \gamma^k d^{k-1} \tag{12}$$

The conjugate coefficient γ is calculated as γ^k

$$\gamma^k = \left(\int_{t=0}^{t_f} \{\nabla S(h^k)\}^2 dt\right) / \left(\int_{t=0}^{t_f} \{\nabla S(h^{k-1})\}^2 dt\right) \tag{13}$$

where is $\overset{o}{\Upsilon} = 0.if\ h' = h^k + d^k$ substituted in heat eq.(2), then values of ΔT will be calculated at the sensor location as follow

$$\Delta T = T(h) - T(h^k) \tag{14}$$

Therefore, the search step size (β) can be obtained as

$$\beta^k = \int_{t=0}^{t_f} (T(x_s, y_s, t; h^k) - Y(t)) \Delta T(x_s, y_s, t; h^k) \, dt \Big/ \int_{t=0}^{t_f} [\Delta T(x_s, y_s, t; h^k)]^2 dt \tag{15}$$

In this method, an iterative procedure is used to estimate the imposed heat transfer coefficient. This iterative method can be summarized by the following equation:

$$h^{k+1} = h^k - \beta^k d^k, \tag{16}$$

where "d" is a conjugate direction and β is the search step size. The computational procedure for the solution of this inverse problem may be summarized as follows:

Suppose h^n is available at iteration n.

Step 1: Solve the direct problem for T.

Step 2: Examine the stopping criterion considering S(h)<α where α is a small-specified number. Continue if is not satisfied.

In this case, the iterations were stopped when the residuals between measured and estimated temperatures are of the same order of magnitude of the measurement errors. That is,

$$|Y(t)-T(X,t)| < \sigma \text{ (i.e. standard deviation)} \quad (17)$$

Step 3: Compute the gradient of the functional ∇S from Eq. (11)

Step 4: Compute the conjugate coefficient γ^k and direction of descent d^k from Eqs. (13) and (14), respectively.

Step 5: Set $\Delta h = d^k$ in heat equation of the problem and solve for calculated ΔT.

Step 6: Compute the search step size β^k from Eq. (15).

Step 7: Compute the new estimation for h^{n+1} from Eq. (16) and return to step 1.

This case study is nonlinear problem. Thus, for calculating gradient of objectivefunction, adjoint equation is needed. The error function S in integral form is also defined as

$$S = \int_{t=0}^{t_f}\int_{x=0}^{L_1}\int_{y=0}^{E} [Y-T]\delta(x-x_s)\delta(y-y_s)dydxdt \quad (18)$$

where Y is measured temperature and β^k is the estimated value at sensor location. In Eq. (18), (x_s and y_s) refer to sensor location and λ(x) is the Dirac delta function. A Lagrange multiplier λ(x,t) comes into picture in the minimization of the function, Eq.(18), because the temperature T(x,t;h) that appears in such function needs to satisfy a constraint, which is the solution of the direct problem. Such Lagrange multiplier, is needed for the computation of the gradient equation (as will be apparent below), is obtained through the solution of a problem adjoint to the sensitivity problem given by Eq. (19). In order to derive the adjoint problem, we write the following extended function:

$$S(T,h) = \int_{t=0}^{t_f}\int_{x=0}^{L_1}\int_{y=0}^{E} [[Y-T]^2\delta(x-x_s)\delta(y-y_s) - \lambda(x,y,t)(\frac{\partial^2 T}{\partial x^2}+\frac{\partial^2 T}{\partial y^2}-\frac{1}{\alpha}\frac{\partial T}{\partial t})]dydxdt \quad (19)$$

Anexpression for the variation *ΔS(h)* of the function S(h) can be developed by perturbing T(x,t) by *ΔT(x,t)* in equation(5).We note that *ΔS(h)* is the directional derivative of S(h) in the direction of the perturbation *Δh* = [$\Delta h_1,..,\Delta h_n$]. Then, by replacing T(x, *t*) by *[T(x. t)+ [T(x,t)+ ΔT (x,t)]* and S(h) by [*S(h)+ΔS(h)*] in eq.(19), subtracting from the resulting expression the original equation (14),and neglecting second order terms, we find

$$\Delta S(T,q) = \int_{t=0}^{t_f}\int_{x=0}^{L_1}\int_{y=0}^{E} [2[T-Y]\ \delta(x-x_s)\delta(y-y_s)\Delta T(x,t)+... \\ ...+\lambda(x,y,t)(\frac{\partial^2(\Delta T)}{\partial x^2}+\frac{\partial^2(\Delta T)}{\partial y^2}-\frac{1}{\alpha}\frac{\partial(\Delta T)}{\partial t})]dydxdt \quad (20)$$

The second integral term on the right-hand side of this equation is simplified by integration by parts and by utilizing the boundary and initial conditions of Eq. (9). After some manipulation, the adjoint differential equations are obtained as

$$\lambda_{xx}+\lambda_{yy}+2\sum_{i=1}^{N_s}(T-Y)\delta(x-x_i)\delta(y-y_i) = -\lambda_t/\alpha \\ \lambda_{x|x=0} = \lambda_{x|x=l} = 0 and \lambda(t_f) = 0 \\ \lambda_{y|y=0} = 0 and -k\lambda_{y|y=E} = (h+4\varepsilon\sigma T^3(x,E,t))\lambda \\ df = dL = \frac{\partial L}{\partial h}dh \Rightarrow \nabla f = -\lambda(x,E,t)(T(x,E,t)-T_{jet})/k \quad (21)$$

Note that in the adjoint problem, the condition *(λ(t_f))* is the value of the function *λ(x, t)* at the final time $t = t_f$. Thus, this equation must be solved backward.The gradient of the objective function is obtained from the adjoint equations.

In this method, only temperatures history in target plate were recorded by thermocouples.Local convective heat transfer coefficients were estimated by the above mentioned method.

RESULTS AND DISCUSSION

The inverse problem is solved for three different desired Nusselt numbers on the target surface (Nu=7, 9, 11). Convergence histories of the objective function and distributions of local Nusslet number at optimal conditions for Nu=11 are shown in Fig. 4a.

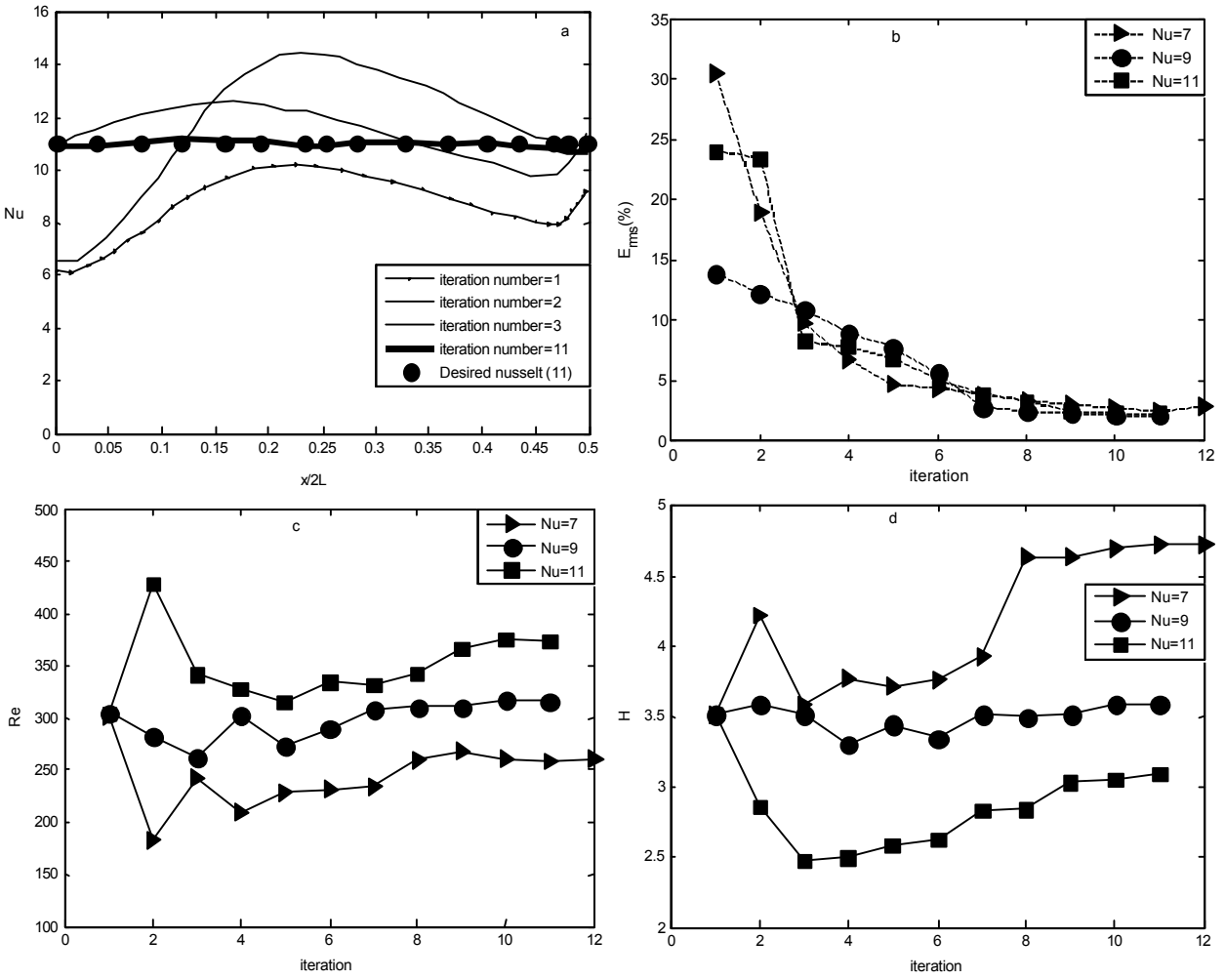

Fig. 4: Convergence history of local Nusselt number and Erms for Nu=11, Convergence history of b) Erms c) Reynolds number and d) H

Table 1: Initial and optimal non-dimensional design variables

	Nu=7		Nu=9		Nu=11	
	Initial	Optimal	Initial	Optimal	Initial	Optimal
Re	303.4	260.12	303.4	317.13	303.4	373.04
W1	0.5	0.356	0.5	0.3356	0.5	0.3196
W2	0.5	0.64	0.5	0.664	0.5	0.68
g1	0.4	0.2928	0.4	0.2394	0.4	0.1684
g2	0.4	0.484	0.4	0.348	0.4	0.239
H	3.5	4.724	3.5	3.6	3.5	3.037
Erms(%)	29.91	2.39	14.04	2.041	23.71	2

These plots show that the convergence has been achieved after at most 12 iterations and the root mean square error is reduced to 2.39%, 2.04% and 2.00% for Nu=7, Nu=9 and Nu=11, respectively (Fig.4b). Thus, the distribution of the local Nusselt number is sufficiently uniform for most engineering applications.

Values of non-dimensional design variables at the initial and optimum conditions are summarized in Table 1 and their convergence histories are plotted in Figs. (4c, 4d and 5 (a-d)). The same initial guesses, i.e., half value of the upper bounds stated in Eq. (8), are used for all three desired Nusselt numbers to prove that the root mean

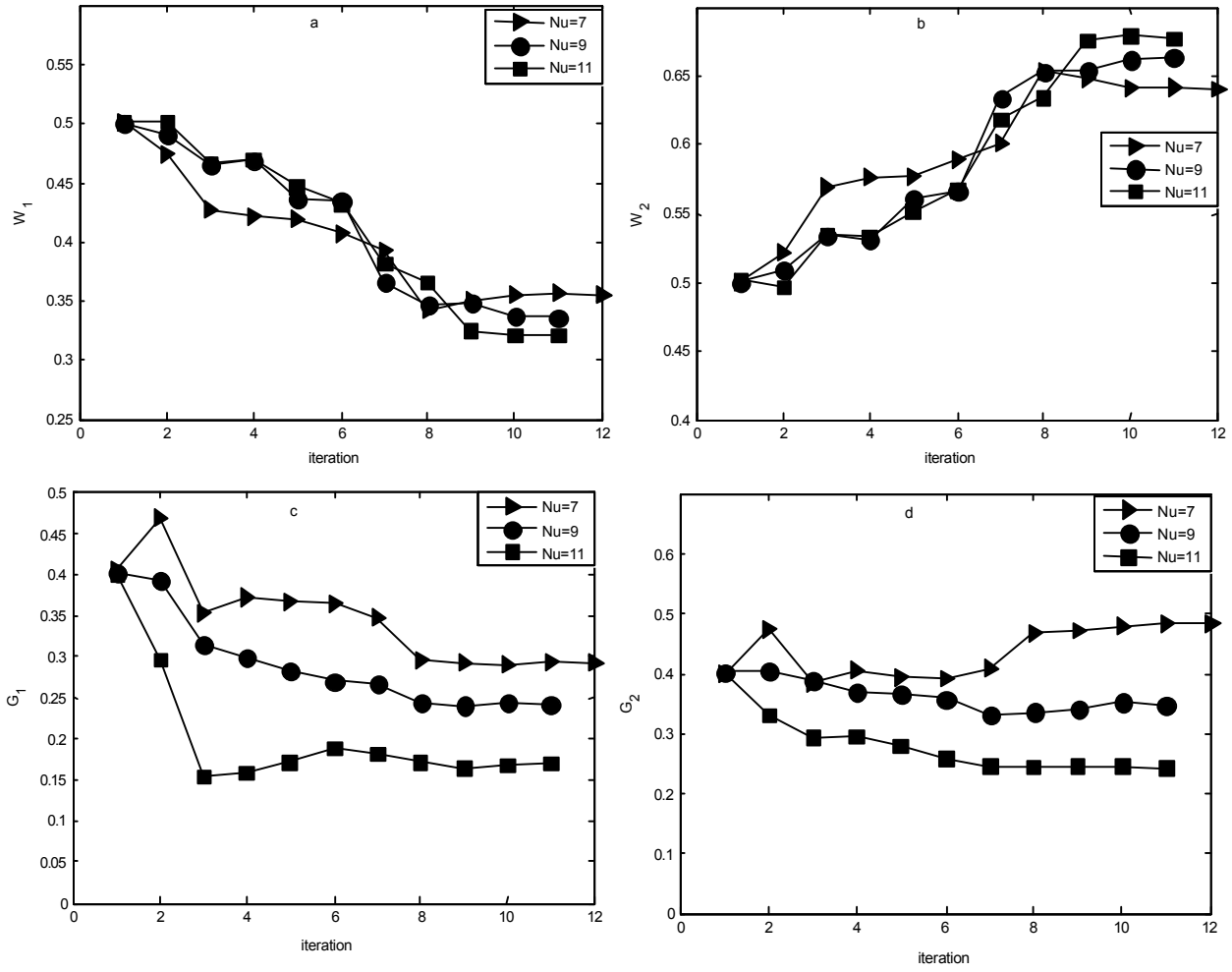

Fig. 5: Convergence history of a) W_1, b) W_2, c) G_1 and d) G_2

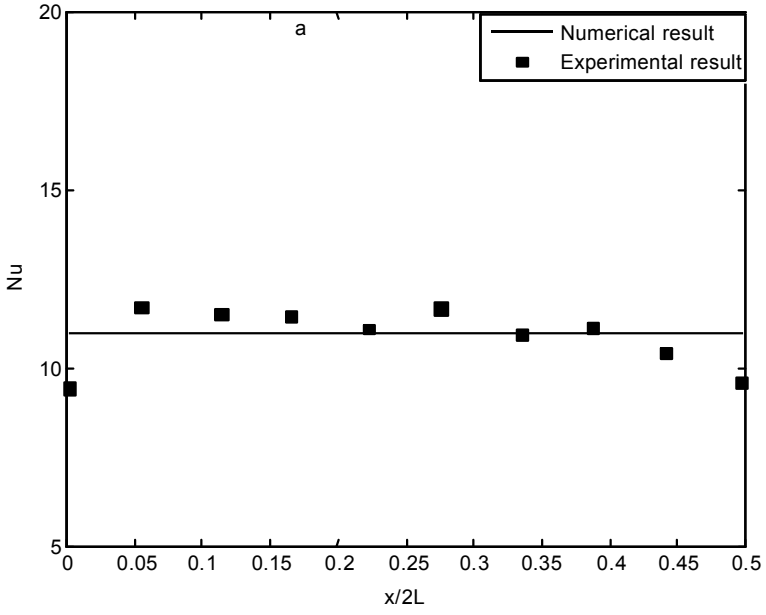

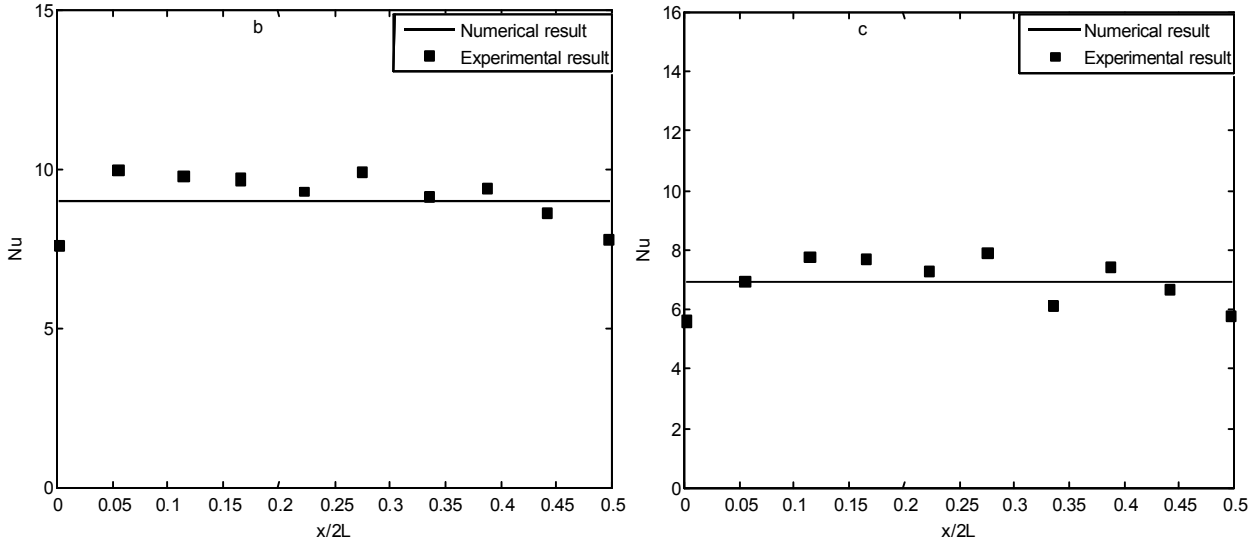

Fig. 6: Experimental and numerical local Nusselt distribution for a) Nu=7, b) Nu=9, c) Nu=11

square error can be reduced significantly in spite of initial values of the design variables. Since the objective function is highly nonlinear, number of iterations for achievement of the uniform Nusselt distribution as well as the values of the optimal design variables depend on the initial guesses.

It is observed that Higher desired Nusselt number leads to higher Reynolds numbers and smaller gap sizes. The second jet width and gap size are larger than the first ones for all three cases. However, the first jet width decreases by increasing the Nusselt number, while the second jet width increases. Jet-to-plate spacing to the hydraulic diameter ratios are inversely proportional to the Nusselt numbers. On the other hand, aforementioned ratio diminishes by rising the Nusselt number.

With attention to the above mentioned experimental method in estimation heat transfer coefficient, Fig. 6 represents the experimentally obtained distribution of local Nusselt number which apparently is in good agreement with the results of the numerical algorithm. Thus, the numerical scheme is successfully validated. Experimental result with numerical result have 11% error. In another points, this is attributed to difference in the thermal boundary condition used, different levels of experimental uncertainty and method.The maximum difference with experimental results occurs in the impingement region and increases with the Reynolds number. These can be attributed to the laminar flow assumption in the CFD simulations.

CONCLUSION

In this research a numerical algorithm was developed in order to obtain an optimal configuration of four planar impinging slot jets to produce uniform heat flux on flat plate. The conjugate gradients optimization method along with backtracking line search was employed to minimize the root mean square deviation of the local Nusselt distribution calculated by CFD simulations from the given Nusselt number. The root mean square error was less than 2.5% for three cases of Nu=7, 9 and 11. Also, an experimental study was performed by using inverse heat transfer method. This method is simple and efficient. In this experimental method, temperatures history in target plate was recorded and using conjugated gradient method with adjoint equation estimate heat transfer coefficient. Radiation heat transfer and lateral heat conduction was considered in this method. The measured Nusselt number for the optimal jet arrangement was in good agreement with the numerical results.

Nomenclature:

E plate thickness (m)
h heat transfer coefficient (W/m^2K)
k thermal conductivity (W/m.K)
L plate length (m)
M time index
N number of discrete measurements
Np number of unknown parameters

Ns number of sensors
P pressure(Pa)
q heat flux vector (W/m^2)
T temperatures (K)
u X-velocity (*m/s*)
v y-velocity (*m/s*)
W slot width (m)
x, y space coordinates
Y measured temperatures (K)

Greek Symbols

Greek Symbols

α thermal diffusivity (m^2/s)
σ standard deviation of noise
β search step size
ε surface emissivity coefficient
γ conjugate coefficient

REFERENCES

1. Roetzel, W. and M. Newman, 1975. "Uniform Heat Flux in a Paper Drying Drum with a Non-cylindrical Condensation Surface Operating under Rimming Conditions," International Journal of Heat and Mass Transfer, 18(4): 553-557.
2. Sparrow, E.M. and C.K. Carlson, 1987. "Experimental Investigation of Heat Flux Uniformity at Thin, Electrically Heated Metallic Foils," International Journal of Heat and Mass Transfer, 30(3): 601-604.
3. Birla, S.L., S. Wang, J. Tang and G. Hallman, 2004, "Improving Heating Uniformity of Fresh Fruit in Radio Frequency Treatments for Pest Control," Postharvest Biology and Technology, 33(2): 205-217.
4. Rafidi, N. and B. Wlodzimierz, 2006. "Heat Transfer Characteristics of HiTAC Heating Furnace Using Regenerative Burners," Applied Thermal Engineering, 26(16): 2027-2034.
5. Zareifard, M.R., M. Marcotte and M. Dostie, 2006. "A Method for Balancing Heat Fluxes Validated for a Newly Designed Pilot Plant Oven," Journal of Food Engineering, 76(3): 303-312.
6. Chandler, S. and A. Ray, 2007. "Heat Transfer Characteristics of Three Interacting Methane Air Flame Jets Impinging on a Flat Surface," International Journal of Heat and Mass Transfer," 50(3-4): 640-653.
7. Martin, H., 1977. "Heat And Mass Transfer Between Impinging Gas Jets And Solid Surfaces," Advances in Heat Transfer, 13: 1-59.
8. Zuckerman, N. and N. Lior, 2006. "Jet Impingement Heat Transfer: Physics, Correlations and Numerical Modeling," Advances in Heat Transfer, 39: 565-631.
9. Gardon, R. and J.C. Akfirat, 1966. "Heat Transfer Characteristics of Impinging Two-dimensional Air Jets," ASME Journal of Heat Transfer, 88(1): 101-107.
10. Huber, A.M. and R. Viskanta, 1994. "Effect of Jet-Jet Spacing on Convective Heat Transfer to Confined, Impinging Arrays of Axisymmetric Air Jet," International Journal of Heat and Mass Transfer, 37(18): 2859-2869.
11. Wadsworth, D. and I. Mudawar, 1990. "Cooling of a Multichip Electronic Module by Means of Confined Two-Dimensional Jets of Dielectric Liquid," ASME Journal of Heat Transfer, 112(4): 891-898.
12. Wang, L., B. Sundén, A. Borg and H. Abrahamsson, 2011. "Control of jet impingement heat transfer in crossflow by using a rib," International Journal of Heat and Mass Transfer, 54(19-20): 4157-4166.
13. Na-pompet, K. and W. Boonsupthip, 2011. "Effect of a narrow channel on heat transfer enhancement of a slot-jet impingement system," Journal of Food Engineering, 103(4): 366-376.
14. San, J.Y. and J.J. Chen, 2014. "Effects of Jet-to-jet Spacing and Jet Height on Heat Transfer Characteristics of an Impinging Jet Array," International Journal of Heat and Mass Transfer, 71: 8-17.
15. Xing, Y. and B. Weigand, 2013. "Optimum Jet-to-Plate Spacing of Inline Impingement Heat Transfer for Different Crossflow Schemes," ASME Journal of Heat Transfer, 135(7).
16. Versteeg, H.K. and W. Malalasekera, 2007. "An introduction to computational fluid dynamics-the finite volume method," Pearson, England, ISBN: 978-0131274983.
17. Patankar, S.V., 1980. "Numerical heat transfer and fluid flow," McGraw Hill, New York, USA, ISBN: 978-0-89116-522-4.
18. Alifanov, O.M., 1994. Inverse heat transfer problems, Moscow, Russia, Chap. 6. ISBN-13: 978-3-642-76438-7.
19. Woodburry, K.A., 2003. Inverse engineering handbook, Boca Raton, Florida, USA, Chap. 3. ISBN-13: 978-0849308611.
20. Hestenes, M.R. and E. Stiefel, 1952. "Methods of Conjugate Gradients for Solving Linear Equations," Journal of Research of the National Bureau of Standards, 49(6): 409-436.
21. Fletcher, R. and C.M. Reeves, 1964. "Function Minimization by Conjugate Gradients," The Computer Journal, 7(2): 149-154.

22. Nocedal, J. and S.J. Wright, 1999. Numerical Optimization. Springer Verlag, USA, Chap, pp: 3.

23. Farahani, S.D. and F. Kowsary, 2014. Direct estimation local convective boiling heat transfer coefficient in mini channel, Int. Communication Heat and Mass Transfer, 39(2): 304-310.